

Molecular Physics

An International Journal at the Interface Between Chemistry and Physics

ISSN: (Print) (Online) Journal homepage: <https://www.tandfonline.com/loi/tmph20>


Can third-body stabilisation of bimolecular collision complexes in cold molecular clouds happen?

Zhenghai Yang, Srinivas Doddipatla, Chao He, Shane J. Goettl, Ralf I. Kaiser, Ahren W. Jasper, Alexandre C. R. Gomes & Breno R. L. Galvão


To cite this article: Zhenghai Yang, Srinivas Doddipatla, Chao He, Shane J. Goettl, Ralf I. Kaiser, Ahren W. Jasper, Alexandre C. R. Gomes & Breno R. L. Galvão (2022): Can third-body stabilisation of bimolecular collision complexes in cold molecular clouds happen?, Molecular Physics, DOI: [10.1080/00268976.2022.2134832](https://doi.org/10.1080/00268976.2022.2134832)

To link to this article: <https://doi.org/10.1080/00268976.2022.2134832>

 View supplementary material 

 Published online: 18 Oct 2022.

 Submit your article to this journal 

 Article views: 102

 View related articles 

 View Crossmark data 

Can third-body stabilisation of bimolecular collision complexes in cold molecular clouds happen?

Zhenghai Yang^a, Srinivas Doddipatla^a, Chao He^a, Shane J. Goettl^{ib}, Ralf I. Kaiser^{ib}, Ahren W. Jasper^b, Alexandre C. R. Gomes^{ic} and Breno R. L. Galvão^{ic}

^aDepartment of Chemistry, University of Hawai'i at Manoa, Honolulu, HI, USA; ^bChemical Sciences and Engineering Division, Argonne National Laboratory, Lemont, IL, USA; ^cCentro Federal de Educação Tecnológica de Minas Gerais, CEFET-MG, Minas Gerais, Brazil

ABSTRACT

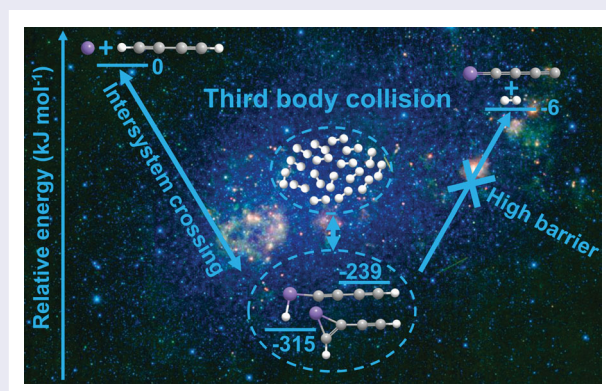
For more than half a century, networks of radiative association, dissociative recombination, and bimolecular reactions have been postulated to drive the low-temperature chemistry of cold molecular clouds. Third-body stabilizations of collision complexes have been assumed to be 'irrelevant' due to short lifetime of such complexes. Here, we conduct crossed molecular beam studies of ground state atomic silicon with diacetylene in combination with electronic structure calculations and microcanonical kinetics models operating under cold molecular cloud conditions. Our combined experimental, electronic structure, and microcanonical kinetics modelling investigations provide compelling evidence that three-body collisions of molecular hydrogen with long-lived reaction intermediates accessed through intersystem crossing are prevalent deep inside molecular clouds. This concept might be exportable to reactions involving polycyclic aromatic hydrocarbons thus affording a versatile machinery to complex organics via third-body stabilizations of bimolecular collision complexes deep inside cold molecular clouds.

ARTICLE HISTORY

Received 18 August 2022
Accepted 7 October 2022

KEYWORDS







Third-body collisions;
silicon-carbon bond; reaction
dynamics; astrochemistry




1. Introduction

Since the discovery of the methylidyne radical (CH) nearly 100 years ago towards the interstellar medium [1,2], cold molecular clouds such as the Taurus (TMC-1) and Orion Molecular Clouds (OMC-1) have been acclaimed as *molecular factories* and *natural laboratories* on a macroscopic scale for developing our fundamental

understanding of the elementary processes driving the molecular synthesis in our universe [3]. An unravelling of these mechanisms on the most fundamental, microscopic level is vital in constraining the cosmic carbon budget [4], in defining the basic elementary reactions that drive the synthesis of complex, often astrobiologically relevant molecules such as sugars and amino acids

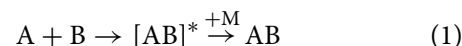
CONTACT Ralf I. Kaiser  ralfk@hawaii.edu  Department of Chemistry, University of Hawai'i at Manoa, Honolulu, HI 96822, USA; Ahren W. Jasper  ajasper@anl.gov  Chemical Sciences and Engineering Division, Argonne National Laboratory, Lemont, IL 60439, USA; Breno R. L. Galvão  brenogalvao@gmail.com  Centro Federal de Educação Tecnológica de Minas Gerais, CEFET-MG, Av. Amazonas 5253, Belo Horizonte, Minas Gerais 30421-169, Brazil

 Supplemental data for this article can be accessed here. <https://doi.org/10.1080/00268976.2022.2134832>

in deep space [5], and in providing a better understanding of the processes which control the formation of Solar Systems including our own. However, with some 250 molecules ranging in complexity from molecular hydrogen (H_2) to the sugar-related glycolaldehyde molecule (HCOCH_2OH) and aromatics such as indene (C_9H_8) [6–8] to fullerenes (C_{60} , C_{70}) [9,10] detected in interstellar and circumstellar environments, even complex reaction networks involving bimolecular ion-molecule [11] and neutral-neutral reactions [12] along with dissociative recombination [12–14] and radiative associations [15–19] have been frequently unsuccessful in accounting for astronomical observations of even major species, such as abundant aromatic molecules like indene (C_9H_8) and organosilicon species like the cyclic silicon dicarbide (SiC_2), with astrochemical models predicting fractional abundances of up to three [8,20] and one order of magnitude lower than astronomically observed [21,22]. This lack of agreement suggests uncharted yet essential fundamental molecular mass growth mechanisms producing complex molecules in deep space [23]. The elucidation of these machineries is vital to eventually comprehend the fundamental processes that affect the lifecycle of carbonaceous and organic matter in our Galaxy. In the outflow of circumstellar envelopes of carbon-rich asymptotic giant branch (AGB) stars, organosilicon molecules such as SiC_n ($n = 1\text{--}4$) represent fundamental molecular building blocks of silicon-carbide dust grains [24–26]. Previously the reaction of the silyldiyne radical (SiH) with diacetylene (C_4H_2) was investigated and the formation of 1-ethynyl-3-silacyclopropenylidene molecule (SiC_4H_2) was confirmed; this species might be ultimately photolyzed to the silicon tetracarbide (SiC_4) molecule [25].

Here, by exploiting crossed molecular beam studies of ground state atomic silicon ($\text{Si}(^3\text{P})$) with diacetylene (C_4H_2) and combining these results with electronic structure calculations along with microcanonical kinetics models operating under cold molecular cloud conditions, we report on the role of non-adiabatic dynamics in the impending third-body stabilisation of long-lived bimolecular collision complexes in the gas phase deep inside cold molecular clouds. Third-body collisions are collisions that stabilise transient reaction intermediates $[\text{AB}]^*$ formed from bimolecular collisions of the reactants A and B via an inert species M. Molecular hydrogen is an abundant constituent of molecular clouds (reaction (1)), but third-body collisions involving molecular hydrogen ($M = \text{H}_2$) have been previously believed to be irrelevant in cold molecular clouds. This is because traditional lifetimes of bimolecular collision complexes $[\text{AB}]^*$ are in the order of picoseconds, which are too short to allow significant stabilisation via a third body

collision [27].



This reaction represents a benchmark and prototype system of a barrierless bimolecular reaction accessing long-lived singlet $[\text{SiC}_4\text{H}_2]^*$ collision complexes, as detected here in molecular beam experiments. This reaction proceeds via non-adiabatic chemical dynamics involving intersystem crossing (ISC) from the initial triplet surface to a lower-energy singlet surface. In the absence of stabilising third-body collisions, the system will eventually re-cross to the triplet surface and re-dissociate back to the reactants; other atomic and molecular hydrogen loss channels are energetically closed. Our microcanonical kinetics model operating under conditions relevant to cold molecular clouds at temperatures of 10 K reveal that up to 12% of all $[\text{SiC}_4\text{H}_2]^*$ complexes can be stabilised via third body collisions with molecular hydrogen where deep inside molecular clouds the number density of molecular hydrogen can be up to 10^8 cm^{-3} . The enhancement of the lifetime of the collision complexes through triplet-singlet crossing and singlet-triplet re-crossing might be exportable to aromatic systems such as those accessed by reactions of ground state carbon atoms ($\text{C}(^3\text{P})$) with polycyclic aromatic hydrocarbons (PAHs) as simple as naphthalene (C_{10}H_8), anthracene ($\text{C}_{14}\text{H}_{10}$), and phenanthrene ($\text{C}_{14}\text{H}_{10}$) with the triplet entrance channel connected to the singlet manifold thus requiring re-crossing to the triplet surface prior to re-dissociation thus affording a previously elusive, versatile mechanism to complex organics via third-body stabilizations of bimolecular collision complexes deep inside cold molecular clouds.

2. Experimental and computational

2.1. Experimental: crossed molecular beams

The gas-phase reaction of ground-state silicon atoms ($\text{Si}; ^3\text{P}$) with diacetylene ($\text{HCCCCH}; \text{X}^1\Sigma_g^+$) was performed under single-collision conditions utilising a crossed molecular beams machine [28]. In the primary source chamber, a pulsed supersonic beam of ground state atomic silicon was generated in situ via laser ablation of a rotating silicon rod ($\text{Si}; 99.999\%$; Goodfellow Corporation) at 266 nm (Nd:YAG; 5 mJ per pulse; 30 Hz) and seeding the ablated atoms in neon carrier gas ($\text{Ne}; 99.999\%$; Airgas; 60 Hz). The primary beam was released by a piezoelectric pulsed valve operating at 60 Hz and a backing pressure of 4 atm. No electronically excited silicon atoms ($\text{Si}; ^1\text{D}$) were present in the primary beam under the experimental conditions

[29]. The atomic silicon beam passed through a skimmer and was then velocity selected by a four-slit chopper wheel rotating at 120 Hz. In the interaction region, the selected section of the silicon beam with a peak velocity (v_p) of $998 \pm 18 \text{ m s}^{-1}$ and speed ratio (S) of 4.6 ± 0.6 crossed perpendicularly with a pulsed diacetylene beam (+99.5%) seeded in argon (99.9999%; AirGas) at a fraction of 5% ($v_p = 630 \pm 20 \text{ m s}^{-1}$, $S = 9.2 \pm 0.3$) and a backing pressure of 550 Torr. This resulted in a collision energy of $12.5 \pm 0.4 \text{ kJ mol}^{-1}$ and centre-of-mass angle of $48.4 \pm 0.5^\circ$. Diacetylene was synthesised in house [30]. The 60 Hz frequency of both pulsed valves and the 30 Hz operation of the laser allows a ‘laser-on’ minus ‘laser-off’ background subtraction.

Scattered species entering the detector were monitored via a triply differentially pumped quadrupole mass spectrometer (QMS) and ionised in an electron-impact ioniser (80 eV, 2 mA). The ions are then filtered according to mass-to-charge (m/z) ratio; ions that passed through the filter are collected by a Daly-type time-of-flight detector. The detection region is housed in a triply differentially pumped, rotatable ultrahigh vacuum chamber at typical pressures of 6×10^{-12} Torr. The TOF spectra collected at different angles were integrated and normalised with respect to the intensity at the CM angle to extract the laboratory angular distribution at a specific m/z ratio. To obtain information on the chemical dynamics, the laboratory data were transformed into the CM reference frame using a forward-convolution routine [31]. The user-defined angular $T(\theta)$ and translational energy $P(E_T)$ flux distribution are varied iteratively until a best fit of the laboratory TOF spectra and angular distribution is reached.

2.2. Computational: electronic structure calculations

The electronic structure calculations were carried out using the GAMESS [32] and MOLPRO [33] packages. As a first step, we explored the singlet and triplet potential energy surfaces (PESs) of the SiC_4H_2 system with the wB97X-D functional [34] with the pcseg-2 basis set [35]. With this method, we have located several minima and saddle points (SPs) on the PESs and performed a harmonic vibrational analysis for each of them, from where the zero-point energies (ZPE) were extracted. For all SPs, an intrinsic reaction coordinate calculation was performed to ensure the proper connections pathways. We have also identified crossings between singlet and triplet electronic states and have located their minimum energy on the seam of intersection (MSX). These structures are not simple stationary structures, and a normal vibrational analysis is not possible. To extract their

ZPE, we have employed an effective Hessian, following the procedure outlined in references [36–38]. Briefly, we first calculate the gradient and the conventional Hessian matrix of the singlet and triplet PESs independently at the geometry of the MSX. To generate the effective Hessian matrix, the coordinate perpendicular to the seam is projected out along with the translational and rotational degrees of freedom. The new Hessian matrix is then diagonalised to yield the $3N-7$ vibrational frequencies of the MSX, using the implementation of Ganon and coworkers [39]. After this initial exploration of the PESs, we refined the energies for each of the structures by performing single point energy calculations using the explicitly correlated CCSD(T)-F12 method [40,41] with the cc-pVTZ-F12 basis set [42]. All energy values reported in this work are ZPE corrected and are hereafter referred as CCSD(T)-F12/aug-cc-pVTZ-F12//wB97X-D/pcseg-2 + ZPE(wB97X-D/pcseg-2).

2.3. Computational: microcanonical kinetics model

Isomerisation kinetics for transitions with saddle points were calculated using conventional transition state theory (TST) and rigid rotor/ harmonic oscillator state counts using the electronic structure information computed above. Kinetics for intersystem crossing were calculated similarly using the properties of the minimum energy points on the crossing seams along with the double passage Landau–Zener approximation [43–45]. As reviewed by Harvey [44], this approach which is sometimes called nonadiabatic TST (NA-TST), involves rate equations that appear similar to conventional TST but with an additional integral over a nonadiabatic transition probability. NA-TST was used to generate microcanonical fluxes connecting singlet and triplet wells as indicated in Figure 3, and these spin-forbidden fluxes were used in the kinetic model alongside TST fluxes for the conventional spin-allowed transition states. Finally, the barrierless kinetics for ${}^3\text{Si} + \text{C}_4\text{H}_2$ capture were calculated using variable reaction coordinate (VRC)-TST [46] at the CASPT2/aug-cc-pVTZ level of theory. Microcanonical rate constants $k_i(E)$ were calculated for the forward and reverse reactions for each of these transition states and crossing seams i , where the total energy is defined relative to the separated reactants. These microcanonical rate constants $k_i(E)$ were exploited then to solve a time-dependent master equation via straightforward propagation to describe the populations of the energetically accessible wells. Results were found to be insensitive to the ‘dead end’ wells (T3–T4; S4–S6), and these were omitted from the model to allow for larger integration timesteps, leaving T1, T2, S1, S2, and S3. The results were also found to be insensitive to the partitioning of the

initial population, as the steady state is established on the order of hundreds of nanoseconds, whereas the lifetimes of interest here are more than three orders of magnitudes larger. The rate of production of $^3\text{Si} + \text{C}_4\text{H}_2$ was monitored, and its exponential rate of production gives the desired dissociation rate constant k_d .

3. Results

3.1. Crossed molecular beam studies

The crossed molecular beam experiments of ground-state atomic silicon (Si ; ^3P) with diacetylene (HCC-CCH ; $X^1\Sigma_g^+$) were carried out at a collision energy of $12.5 \pm 0.4 \text{ kJ mol}^{-1}$ (Supplementary material). Considering the natural isotope abundances of silicon (^{28}Si , 92.2%; ^{29}Si , 4.7%; ^{30}Si , 3.1%) and carbon (^{12}C , 98.9%; ^{13}C , 1.1%), signal was searched for from $m/z = 80$ ($^{30}\text{SiC}_4\text{H}_2^+$) to 76 ($^{28}\text{SiC}_4^+$). Ion counts at $m/z = 76$ ($^{28}\text{SiC}_4^+$), 78 ($^{30}\text{SiC}_4^+$, $^{29}\text{Si}^{13}\text{CC}_3^+$, $^{29}\text{SiC}_4\text{H}^+$, $^{28}\text{Si}^{13}\text{CC}_3\text{H}^+$, $^{28}\text{SiC}_4\text{H}_2^+$), and 79 ($^{30}\text{SiC}_4\text{H}^+$, $^{29}\text{Si}^{13}\text{CC}_3\text{H}^+$, $^{29}\text{SiC}_4\text{H}_2^+$, $^{28}\text{Si}^{13}\text{CC}_3\text{H}_2^+$) were accumulated at levels of $19 \pm 2\%$, $22 \pm 2\%$ and $6 \pm 1\%$ compared to signal at 77 ($^{29}\text{SiC}_4^+$, $^{28}\text{Si}^{13}\text{CC}_3^+$, $^{28}\text{SiC}_4\text{H}^+$) (Figures 1 and 2). It is important to note that the time-of-flight (TOF) spectra recorded from $m/z = 79$ to 76 are identical after scaling suggesting the existence of a single channel (Figure S1). However, our electronic structure calculations revealed that the atomic hydrogen loss channel forming the thermodynamically most stable 1,3-butadiynylsilyl (SiCCCCH ; $X^2\Sigma^+$) is endoergic by 58 kJ mol^{-1} and hence not accessible considering the collision energy. Further, although the molecular hydrogen loss channel forming silicon tetracarbide isomer 4-silylene-1,2,3-butatrienylidene (SiCCCC ; $X^1\Sigma^+$) is exoergic by 6 kJ mol^{-1} , the exit transition states connecting the SiC_4H_2 reaction intermediates are at least 80 kJ mol^{-1} above the energy of the separated reactants; therefore, the molecular hydrogen loss is closed, too. The absence of the molecular hydrogen loss channel is also supported by the inability to fit the TOF spectra and laboratory angular distribution with products of a mass combination of 76 amu (C_4Si) plus 2 amu (H_2). Therefore, the laboratory data suggest that both the atomic and molecular hydrogen loss channels are absent under our experimental conditions.

Where can signal at $m/z = 76$ –79 arise from? The laboratory data suggest the existence of long-lived SiC_4H_2 adducts ($^{28}\text{SiC}_4\text{H}_2$, 78 amu; $^{29}\text{SiC}_4\text{H}_2$, 79 amu) with lifetimes exceeding their flight time from the collision centre to the electron-impact ioniser of $643 \pm 6 \mu\text{s}$. In this case, signal at $m/z = 76$ and 77 originates from dissociative electron impact ionisation of the SiC_4H_2 adducts in the ioniser. Considering the best signal-to-noise

ratio, TOF spectra were collected at distinct laboratory angles in 2.5° intervals at $m/z = 77$ revealing a forward-backward symmetric, narrow laboratory angular distribution (LAD) centred around the centre-of-mass (CM) angle of $48.4 \pm 0.5^\circ$ (Table S1). To support this hypothesis, the experimental data were transformed from the laboratory to the CM reference frame accounting for the beam velocities, velocity spreads, and apparatus functions[47]. Here, the laboratory data (Figure 1) could be fit with a single-channel forming a SiC_4H_2 adduct via the reaction of Si (28 amu) with C_4H_2 (50 amu). The CM translational energy flux distribution, $P(E_T)$, peaks at only around 1 kJ mol^{-1} . The maximum translational energy E_{max} ($13 \pm 2 \text{ kJ mol}^{-1}$) is in line with the collision energy ($12.5 \pm 0.4 \text{ kJ mol}^{-1}$) (Figure 2). As for adduct formation and detection in crossed molecular beam studies, the centre-of-mass angular distribution was isotropic (flat) [48–50]. Overall, the experimental data provide compelling evidence of the exclusive formation of SiC_4H_2 adducts as the result of a collision of silicon (^3P) with diacetylene; the lifetime of (some of) these adducts has to exceed the flight time of $643 \pm 6 \mu\text{s}$.

3.2. Potential energy surfaces

With the laboratory and CM data affording persuasive testimony on the existence of a long-lived SiC_4H_2 adduct(s) at a collision energy of $12.5 \pm 0.4 \text{ kJ mol}^{-1}$, we transfer these findings now to interstellar environments to evaluate the lifetime and impact in these cold environments at 10 K. To achieve this objective, we first compute the underlying singlet and triplet potential energy surfaces (PESs) for the bimolecular reaction between silicon (Si ; ^3P) and diacetylene (HCCCCH ; $X^1\Sigma_g^+$) along with non-adiabatic processes (intersystem crossing) and excited state dynamics to an accuracy of about 5 kJ mol^{-1} . Thereafter, a microcanonical kinetics model for the spin-orbit coupled singlet and triplet surfaces is constructed from electronic structure, transition state theory, and non-adiabatic kinetics calculations; the computed microcanonical rate constants were exploited to solve a time-dependent master equation describing the populations of the energetically accessible reaction intermediates in Figure 3 (Figure S2, Table S2). This strategy allows assessing the impact of the collision energy and temperature on the overall reaction mechanism(s) and lifetimes of distinct SiC_4H_2 adducts and to generalise the laboratory result to conditions in the interstellar medium.

The electronic structure calculations identified seventeen reaction intermediates on the triplet (**T1-T6**) and singlet surfaces (**S1-S11**) along with transition states connecting these intermediates via hydrogen migration, ring-opening, and ring-closures as well as exit transition

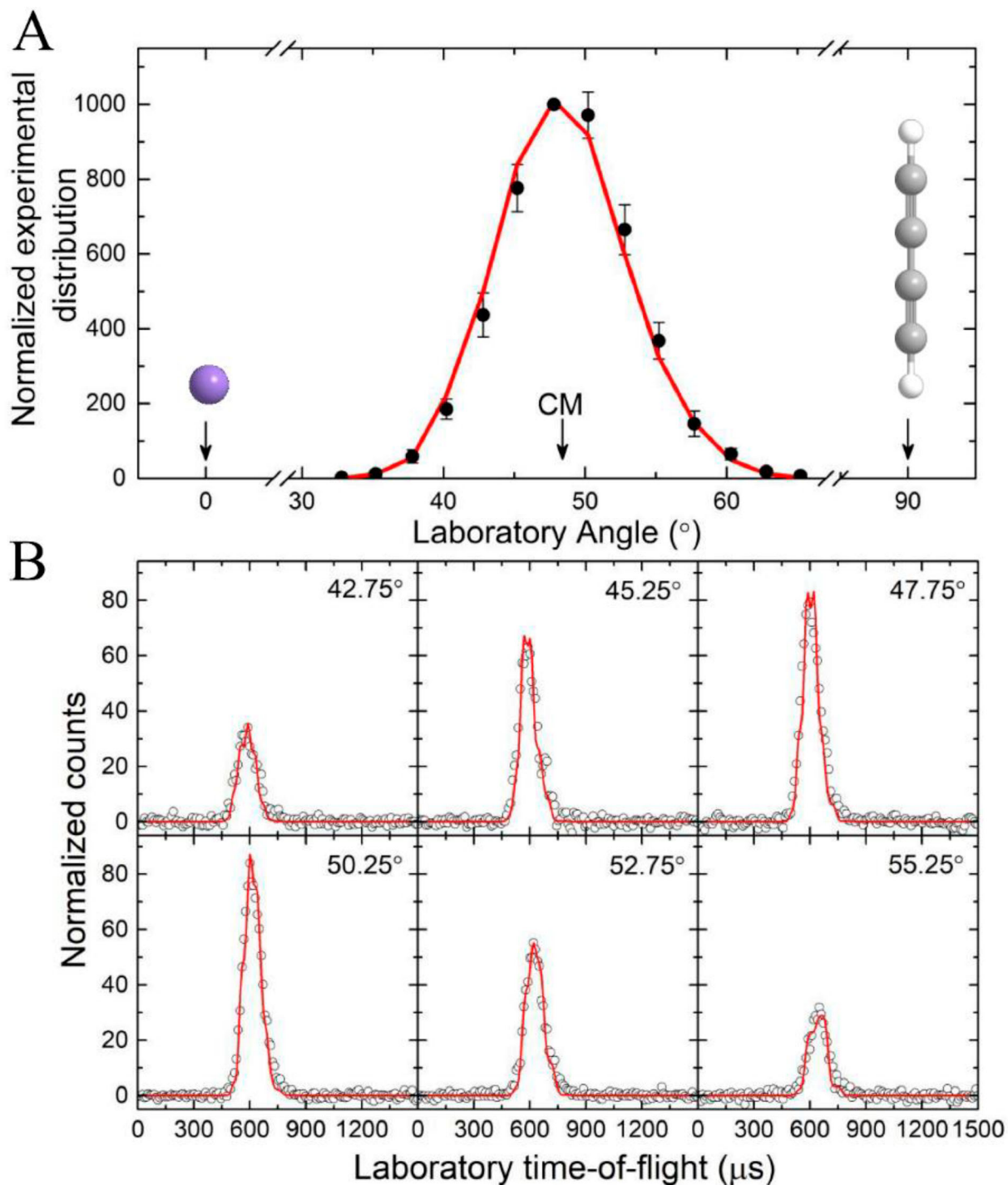


Figure 1. Laboratory angular distribution (A) and time-of-flight spectra (B) are recorded at $m/z = 77$. The solid circles with their error bars represent the normalised experimental distribution; the open circles indicate the experimental data. The red lines represent the best fits obtained from the optimised centre-of-mass (CM) functions, as depicted in Figure 2. Colours of the atoms: silicon, purple; carbon, grey and hydrogen, white.

states for molecular and atomic hydrogen losses leading to SiC_4 (**p1**, **p4**) and SiC_4H (**p2**, **p3**) reaction products, respectively. At the collision energy of interest of $12.5 \pm 0.4 \text{ kJ mol}^{-1}$, just four triplet (**T1-T4**) and six singlet (**S1-S6**) intermediates are energetically accessible. Although the remaining intermediates reside in potential

energy wells and are bound with respect to the energy of the separated reactants, these intermediates are separated from **T1-T4** and **S1-S6** by transition states exceeding the experimental collision energy and, hence, are energetically not reachable. In detail, on the triplet surface, ground state atomic silicon adds barrierlessly to one of

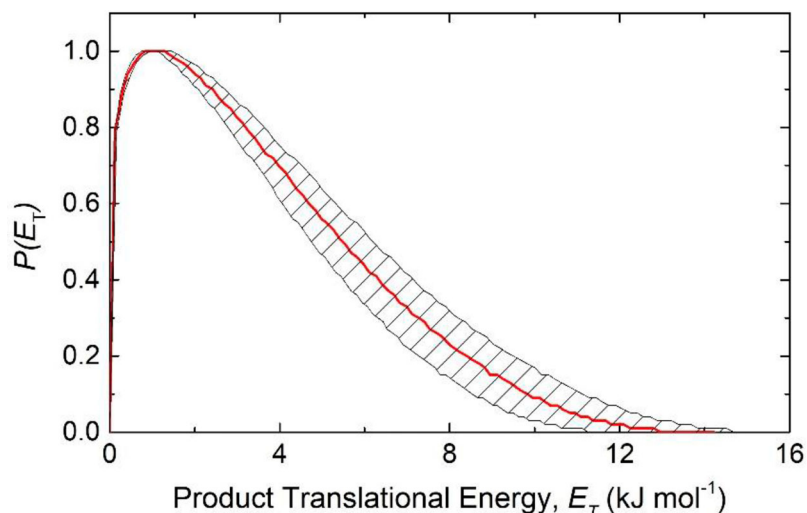


Figure 2. Centre-of-Mass (CM) translational energy flux distribution of the Si-C₄H₂ reaction. Shaded areas indicate the error limits of the fits; the red solid lines define the best-fit functions.

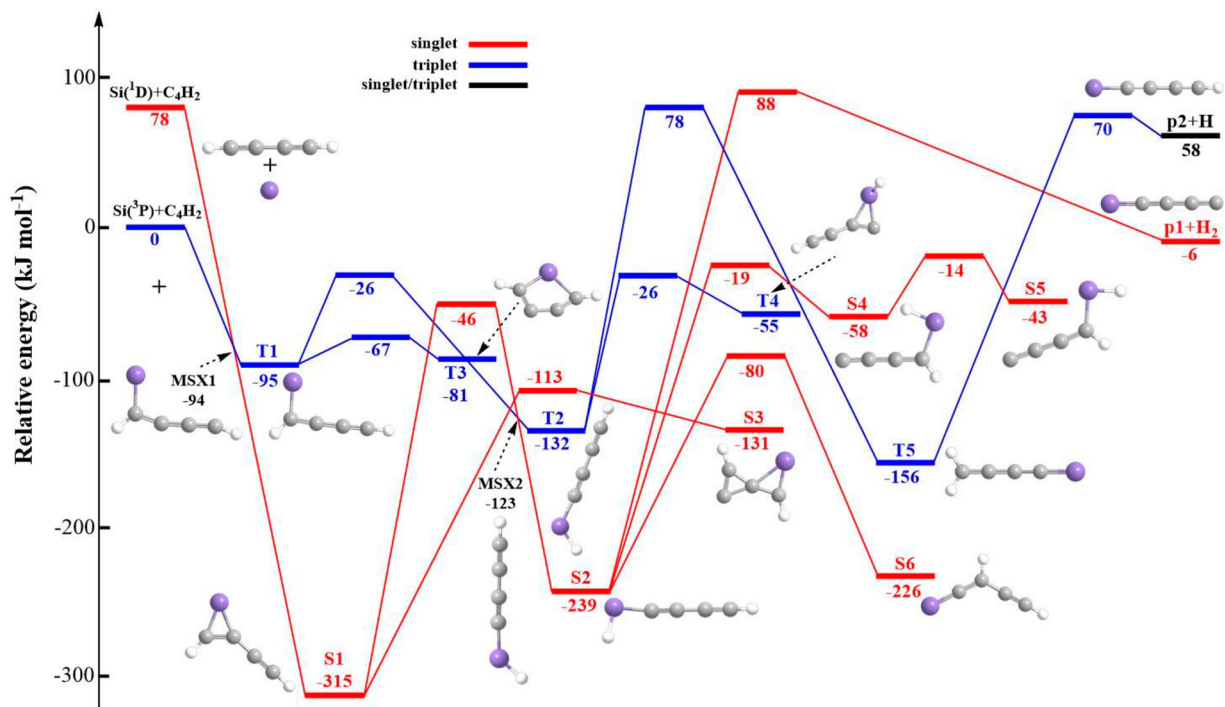


Figure 3. Singlet and triplet potential energy surfaces (PES) along with minima on the seam of crossings (MSX). Cartesian coordinates and vibrational frequencies of reactants, intermediates, transition states, and products are compiled in the Supplementary material.

the terminal carbon atoms of the ethynyl moiety forming the acyclic, C_s symmetric intermediate **T1**. The latter can isomerise via a hydrogen shift from the carbon to the silicon atom or through cyclisation to intermediates **T2** and **T3**, respectively. **T2** may undergo ring-closure to **T4**. The ground state of the atomic silicon is a triplet and therefore the reaction initially proceeds on the triplet surface, but the singlet adducts **S1** and **S2** are lower in energy than the triplet ones. This causes the singlet and triplet surfaces to cross one another at a geometry close

to that of the triplet adducts **T1** and **T2** connecting to **S1** and **S2**, respectively. The local minima on this seam of crossings (MSX) are labelled as **MSX1** and **MSX2**. Similar spin orbit coupling matrix elements were computed for the two crossing seams (53.6 and 44.0 cm⁻¹ for **MSX1** and **MSX2**, respectively, computed using Molpro's implementation of the Breit-Pauli model [51] at the CASSCF/cc-pVTZ level of theory). Note that inter-system crossing (ISC) from **T1** to **S1** is accompanied by a ring closure to the C_s symmetric **S1** intermediate

2-ethynyl-silacyclopropenylidene, which represents the global minimum of the SiC_4H_2 PES. **S1** and **S2** are connected through a transition state barrier 46 kJ mol^{-1} below the energy of the separated reactants; **S3**, **S4**, **S5**, and **S6** can be accessed via ring closure, hydrogen migration, cis-trans isomerisation, and hydrogen shift, respectively. However, none of the reaction intermediates can undergo unimolecular decomposition via molecular or atomic hydrogen losses to SiC_4 (**p1**, **p4**) and SiC_4H (**p2**, **p3**), respectively. Although the overall formation of 4-silylene-1,2,3-butatrienylidene (**p1**; SiC_4CCC ; $X^1\Sigma^+$) plus molecular hydrogen is exoergic by 6 kJ mol^{-1} , even the energetically most favourable transition state connecting intermediate **S2** to **p2** resides 88 kJ mol^{-1} above the energy of the separated products and, hence, is energetically not accessible. Likewise, atomic hydrogen loss channels to 1,3-butadiynylsilyl (**p2**; SiCCCCCH ; $X^2\Sigma^+$) and 2-ethynyl-silacycloprop-2-en-1-ylidene (**p3**; $c\text{-SiCCCCCH}$; X^2A') are endoergic by 58 and 100 kJ mol^{-1} , respectively, and hence are closed, too. Therefore, neither atomic nor molecular hydrogen loss channels are energetically open neither under our experimental conditions nor in the cold interstellar medium (10 K).

3.3. Microcanonical kinetics model

A microcanonical kinetics model for the spin-orbit coupled singlet and triplet surfaces was developed from the electronic structure calculations to characterise the lifetime of the singlet adducts once they are formed via ISC under experimental conditions mimicking the crossed molecular beam study and in the low temperature conditions of cold molecular clouds (10 K). In detail, the microcanonical kinetics model reveals that at the collision energy of 12.5 kJ mol^{-1} , populations of the adducts are primarily distributed between **S1** and **S2** with negligible populations of less than 2×10^{-3} in the triplet wells **T1** and **T2** (Figure 4). Upon collision between triplet silicon and diacetylene, the transient **T1** adduct is formed, which then produces **S1** via ISC mediated by **MSX1**. Notably, intersystem crossing to the singlet states dominates the branching for both **T1** and **T2**, which leads to rapid equilibration among the lower-energy longer-lived singlet wells and the transient triplet wells. The singlet adducts **S1** and **S2** cannot undergo unimolecular decomposition on the singlet surface to electronically excited silicon atoms ($\text{Si}(^1\text{D})$) plus diacetylene since the overall pathway is effectively endoergic by 78 kJ mol^{-1} .

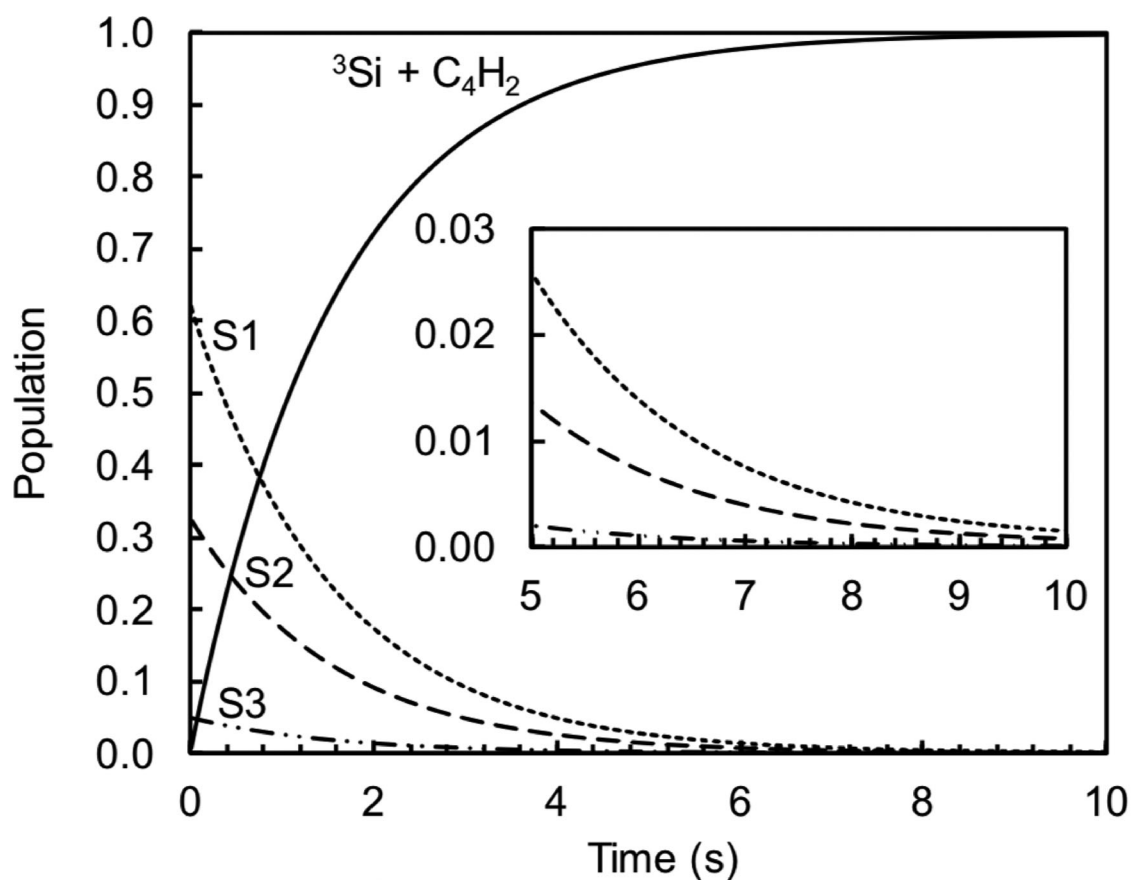


Figure 4. Time-dependent populations. The populations are calculated using a microcanonical kinetics simulation for the experimental collision energy of 12.5 kJ mol^{-1} ; the triplet wells have populations too low to be visible ($< 2 \times 10^{-3}$).

Consequently, in order to decompose, the adducts **S1** and **S2** have to cross back from the singlet to the triplet surface prior to unimolecular fragmentation to ground state silicon plus diacetylene. Therefore, the triplet–singlet crossing and singlet–triplet re-crossing is fundamental and central to establishing the decomposition rates of the adducts. Overall, the loss of the adducts and re-emerging of the reactants is visualised in Figure 4 along with the time-dependent populations of the **S1**, **S2** and **S3** adducts; recall that the triplet wells have populations too low to be visible at a level of less than 2×10^{-3} . Any population that ‘visits’ T1 or T2 is rapidly either recycled back to the singlets or, less frequently, dissociates to $\text{Si}(^3\text{P}) + \text{diacetylene}$. The collision energy dependent half-life $t_{1/2}(E)$ is related to the decomposition rate k_d via $t_{1/2}(E) = \ln(2)/k_d(E)$. At the experimental collision energy, the microcanonical master equation simulations predict a half-life of $t_{1/2} = 108 \mu\text{s}$. A population analysis using this computed half-life reveals that 1–2% of the adducts survive the flight time of $643 \mu\text{s}$ from the collision centre in the molecular beams machine to the electron-impact ioniser of the detector. This long lifetime may be rationalised by expressing the rate for the re-formation of the reactants (^3Si , C_4H_2) as $\dot{n}_R = k_{\text{T1R}}n_{\text{T1}}$, where n_R and n_{T1} are the populations of the re-formed reactants and intermediate **T1**, respectively, and k_{T1R} is the reverse of the capture rate constant of the reactants to **T1**. At 12.5 kJ mol^{-1} , k_{T1R} is $4.3 \times 10^7 \text{ s}^{-1}$. This corresponds to a half-life of just 0.020 ms suggesting that the rate constant for the bond fission step alone is insufficient to explain the observed half-life. Instead, the long lifetime may be attributed to the small steady state population of the triplet adduct **T1** ($n_{\text{T1}} = 1.5 \times 10^{-4}$), which is a consequence of its rapid equilibration with the much lower-energy singlet complexes accessible via ISC.

3.4. Molecular clouds

Having benchmarked the microcanonical kinetics model with the experimental detection of the SiC_4H_2 adduct, we export this framework to determine the fraction of adducts that can be stabilised via third body collisions with molecular hydrogen deep inside cold molecular clouds at 10 K (Figure 5). Starting from the Maxwell–Boltzmann velocity distribution at 10 K (Figure 5(A)) and computed collision rate constants Z between molecular hydrogen and the adduct, the number of collisions per second, z , at number densities, n , of molecular hydrogen deep inside the core of molecular clouds of $n = 10^8 \text{ cm}^{-3}$ is computed $z = Zn$ at 10 K (Figure 5(B)). Stabilisation requires that the lifetime of the adduct exceeds the time between third-body collisions, $t_{\text{coll}} = 1/z$ (Figure 5(C)). At the maximum in

the Maxwell–Boltzmann distribution, typical collision times of 10 s result, with collision times increasing significantly at lower velocities yielding time scales of 100 s between collisions of the adduct with molecular hydrogen. Figure 5(C) can be converted to the dependence of the time between collisions (t_{coll}) on the collision energy (E) (Figure 5(D)). The decomposition rate of the SiC_4H_2 adducts computed using our kinetic model (k_d) is shown versus the collision energy in Figure 5(E). Putting this all together yields Figure 5(F), which compares collision times t_{coll} with the decomposition half-lives as a function of the collision energy. Typically, the complex lifetimes are shorter than t_{coll} , suggesting inefficient stabilisation, but notably there is some population at low collision energies where this trend is reversed. By integrating branching between these two outcomes over the Maxwell–Boltzmann distributions of collision energies, we can associate up to 12% of the adducts with stabilisation at 10 K and $n = 10^8 \text{ cm}^{-3}$, i.e. at conditions relevant to the centre of cold molecular clouds; this fraction may drop to 1.2% and about 0.1% upon moving away from the core (10^8 cm^{-3}) to regions of $n = 10^7 \text{ cm}^{-3}$ and $n = 10^6 \text{ cm}^{-3}$, respectively. This analysis further supposes that collision-induced stabilisation proceeds with unit efficiency and with an overall collision rate constant Z of about $10^{-9} \text{ cm}^3 \text{ s}^{-1}$. The latter was computed using computed 12–6 Lennard-Jones parameters [52] for the adduct (SiC_4H_2) and molecular hydrogen (H_2) of $\sigma = 411 \text{ pm}$ for the collision diameter and $\varepsilon = 90.96 \text{ cm}^{-1}$ for the dispersion energy. Similar results were computed using a capture model from Troe et al. [53] ($1.1 \times 10^{-9} \text{ cm}^3 \text{ s}^{-1}$) and Klippenstein’s long-range transition state theory [54] ($1.5 \times 10^{-9} \text{ cm}^3 \text{ s}^{-1}$).

4. Discussion and conclusions

The explicit identification of long-lived adducts in the crossed molecular beam reaction of silicon atoms with diacetylene and the implications of these findings to third-body collisions deep inside cold molecular clouds through the exploitation of electronic structure and microcanonical kinetics models have far reaching consequences in understanding the astrochemical evolution of low-temperature interstellar environments. It is believed that radiative association reactions including ion–neutral and neutral–neutral reactions with a typical rate of radiative relaxation of 10^2 – 10^3 s^{-1} are suggested to dominate in the cold interstellar clouds. The model studies predict that the radiative association reaction of ionised atomic carbon (C^+) with molecular hydrogen (H_2) initiates a reaction sequence leading to simple hydrocarbons; radiative association reactions involving the methyl ion (CH_3^+) are thought to be involved in the formation of

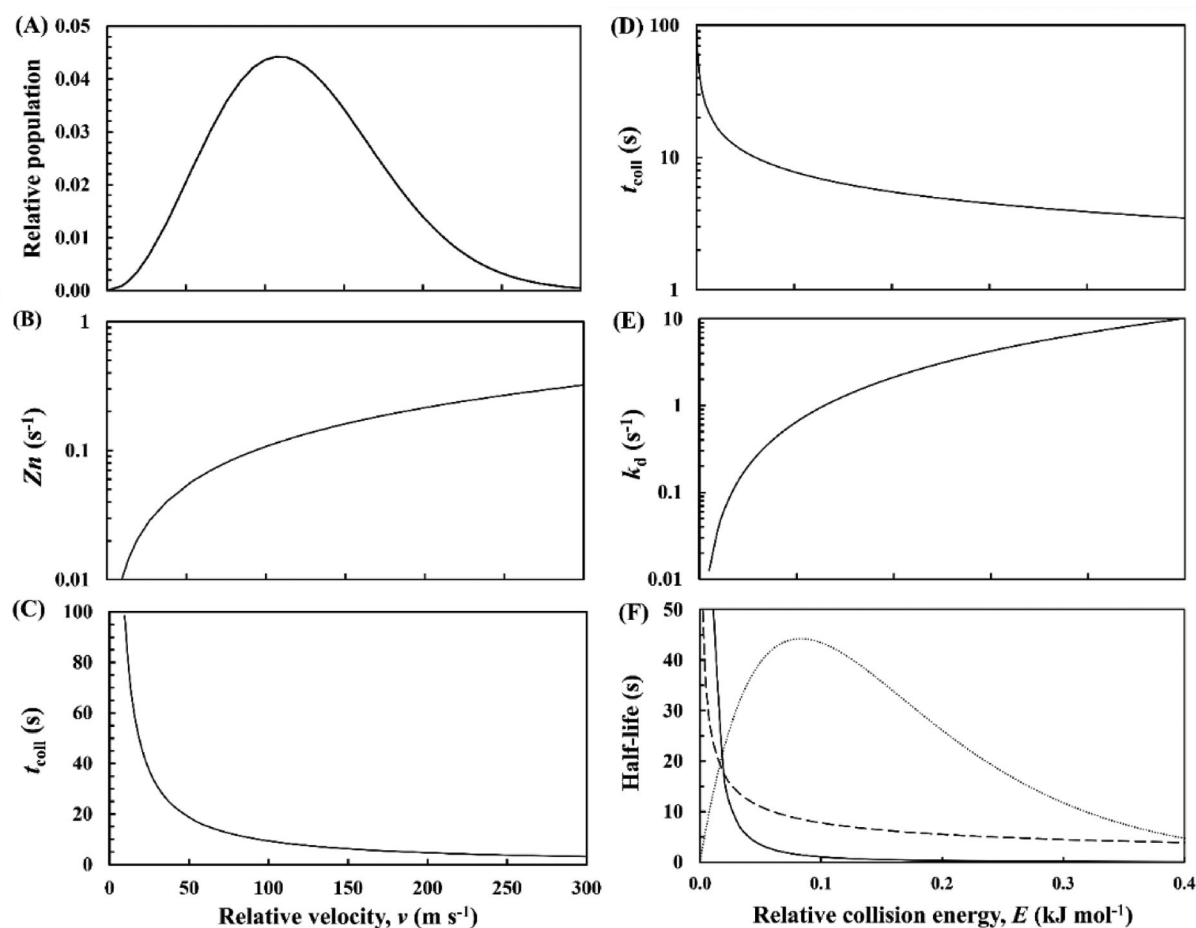


Figure 5. Calculations of fraction of adducts stabilised via third body collisions with H_2 at 10 K. Left: Relative velocity (v) distribution for collisions of atomic silicon with diacetylene at 10 K (A), the total collision rate of the SiC_4H_2 adduct with molecular hydrogen Zn , where Z is the bimolecular collision rate constant and $n = 10^8 \text{ cm}^{-3}$ is the number density of molecular hydrogen (B) and the characteristic collision time t_{coll} (C) versus the relative velocity v . Right: The dependence of t_{coll} (D), the dissociation rate constant k_d (E) on the relative collision energy E and a comparison of the dissociation half-life for the complex $t_{1/2} = \ln(2)/k_d$ (solid line) with t_{coll} (dashed line) along with the relative distribution of collision energies at 10 K (dotted line) (F).

more complex organic species in denser regions [55–57]. Laboratory studies on the radiative association are especially difficult since it can only occur at very low density and very low temperature. To date, only radiative associations via ion-molecule reaction have been studied experimentally. Gerlich et al. measured the association rates for the ion-neutral systems in the ion traps down to very low temperature of 5 K [16,58,59]. During the reaction, the density dependence of the neutral target gas is measured and the results that association experiments are best performed at densities where stabilisation of the collision complex by a third body collision becomes comparable with radiative stabilisation is revealed. In addition, ion-molecule associative reactions were explored by Armentrout et al. using guided ion beam mass spectrometry, which deepen our understanding of ionic structures and reaction dynamics [60–62]. Here, the conceptual framework of a third-body stabilisation of long-lived collision

complexes inside cold molecular clouds suggests that a previously neglected class of chemical reactions – third-body collisions of molecular hydrogen with long-lived reaction intermediates of bimolecular collisions – may influence low-temperature interstellar chemistry. The behaviour of this class of reactions relies on five prerequisites: (i) a barrierless entrance channel from the reactants to the intermediate, (ii) efficient intersystem crossing such as triplet–singlet crossing (non-adiabatic dynamics), (iii) the closure of all exit channels for bimolecular reactions due to reaction endoergicities or energetically insurmountable exit transition states, (iv) re-crossing of the reaction intermediate(s) from the singlet to the triplet surface prior to re-dissociation of the triplet complexes to the initial reactants, and (v) life-time(s) of the reaction intermediate(s) longer than the time between collisions with molecular hydrogen – the dominant molecular component in cold molecular clouds.

Which factors could enhance these prerequisites? *First*, a facile intersystem crossing and efficient spin-orbit coupling (SOC) could be facilitated through the ‘heavy atom effect’ [63,64] and hence barrier-less bimolecular reactions initiated by, e.g. silicon atoms ($\text{Si}(^3\text{P})$) with unsaturated hydrocarbons such as diacetylene as studied here. Although ground state silicon atoms do not react with astronomically abundant C1 to C3 hydrocarbons such as methane (CH_4), acetylene (C_2H_2), ethylene (C_2H_4), methylacetylene (CH_3CCH), allene (H_2CCCH_2), propylene (C_3H_6) and even benzene (C_6H_6) via bimolecular reactions [65], early kinetics experiments by Canosa et al. and Basu and Husain proposed fast reaction rates of up to a few $10^{-10} \text{ cm}^3 \text{ s}^{-1}$ of the reactions of $\text{Si}(^3\text{P})$ with unsaturated hydrocarbons at temperatures as low as 15 K [66,67]. These discrepancies might be reconciled by accounting for a barrierless entrance channel, facile non-adiabatic dynamics along with intersystem crossing from the triplet to the singlet surface, no available bimolecular reactive exit channels, and a re-crossing of the reaction intermediates from the singlet to the triplet surface. These processes could enhance the lifetime of the reaction intermediates so that the organosilicon adducts can be stabilised through a third body with the buffer gas in the CRESU studies thus implicating potential reaction pathways to an organosilicon chemistry in deep space at ultralow temperatures. Note that ‘light’ atoms of the second row of the periodic system of the elements such as ground state atomic oxygen ($\text{O}(^3\text{P})$) also undergo ISC upon reaction with unsaturated hydrocarbons such as methylacetylene (CH_3CCH), allene (H_2CCCH_2), and benzene (C_6H_6) [68–70]; however, these bimolecular reactions have entrance barriers ranging from 6.7 to 15.9 kJmol^{-1} , which cannot be overcome at typical cold molecular cloud temperatures of 10 K. *Second*, the life-time of the intermediates can be enhanced by increasing the availability of oscillators such as low frequency bending fundamentals along with ring deformation and puckering modes such as of polycyclic aromatic hydrocarbons (PAHs) in the interstellar medium [3,71–73]. This could in turn enhance the lifetime of intermediates formed via bimolecular collisions with ground state atomic silicon and potentially the lighter atomic carbon thus providing an unconventional route to previously neglected third-body regimes in deep space.

Overall, our combined experimental, computational, and microcanonical kinetics study represents a first step toward a systematic understanding of the potential role of third-body stabilizations of long-lived collision complexes inside cold molecular clouds. This concept provides a previously elusive, potentially versatile mechanism to complex organics thus bringing us closer in

the elucidation of the fundamental pathways driving the complex chain of reactions toward organic matter on the microscopic, molecular level in our Galaxy.

Acknowledgements

The authors thank Prof. Eric Herbst, University of Virginia, and Dr. Stephen J. Klippenstein, Sandia National Laboratories, for valuable discussions. AWJ gratefully acknowledges computing resources provided by Bebop, a high-performance computing cluster operated by the Laboratory Computing Resource Center at Argonne National Laboratory.

Disclosure statement

No potential conflict of interest was reported by the author(s).

Funding

This work at the University of Hawaii was supported by the U.S. National Science Foundation (CHE-1853541). BRLG acknowledges financial support from Conselho Nacional de Desenvolvimento Científico e Tecnológico (CNPq, grant number 311508/2021-9) and CEFET-MG. AWJ was supported by the U. S. Department of Energy, Office of Basic Energy Sciences, Division of Chemical Sciences, Geosciences, and Biosciences through Argonne National Laboratory. Argonne is a U. S. Department of Energy laboratory managed by UChicago Argonne, LLC, under Contract Number DE-AC02-06CH11357.

ORCID

Shane J. Goettl  <http://orcid.org/0000-0003-1796-5725>

Ralf I. Kaiser  <http://orcid.org/0000-0002-7233-7206>

Alexandre C. R. Gomes  <http://orcid.org/0000-0003-3397-5130>

Breno R. L. Galvão  <http://orcid.org/0000-0002-4184-2437>

References

- [1] T. Dunham, *Publ. Astron. Soc. Pac.* **49**, 26–28 (1937). doi:10.1086/124759
- [2] P. Swings and L. Rosenfeld, *Astrophys. J.* **86**, 483–486 (1937). doi:10.1086/143880
- [3] A.G.G.M. Tielens, *Rev. Mod. Phys.* **85** (3), 1021 (2013). doi:10.1103/RevModPhys.85.1021
- [4] A.G.G.M. Tielens and L.J. Allamandola, *Cool Interstellar Physics and Chemistry* (Jenny Stanford Publishing, New York, 2011), pp. 341–380.
- [5] P. Ehrenfreund and S.B. Charnley, *Annu. Rev. Astron. Astrophys.* **38** (1), 427–483 (2000). doi:10.1146/annurev.astro.38.1.427
- [6] G.R. Carruthers, *Astrophys. J.* **161**, L81 (1970). doi:10.1086/180575
- [7] J.M. Hollis, F.J. Lovas and P.R. Jewell, *Astrophys. J.* **540** (2), L107 (2000). doi:10.1086/312881
- [8] S. Doddipatla, G.R. Galimova, H. Wei, A.M. Thomas, C. He, Z. Yang, A.N. Morozov, C.N. Shingledecker, A.M. Mebel and R.I. Kaiser, *Sci. Adv.* **7** (1), eabd4044 (2021). doi:10.1126/sciadv.abd4044

- [9] J. Cami, J. Bernard-Salas, E. Peeters and S.E. Malek, *Science*. **329** (5996), 1180–1182 (2010). doi:10.1126/science.1192035
- [10] A. Chuvilin, U. Kaiser, E. Bichoutskaia, N.A. Besley and A.N. Khlobystov, *Nat. Chem.* **2** (6), 450–453 (2010). doi:10.1038/nchem.644
- [11] T.R. Geballe and T. Oka, *Nature*. **384** (6607), 334–335 (1996). doi:10.1038/384334a0
- [12] R.I. Kaiser, C. Ochsenfeld, M. Head-Gordon, Y.T. Lee and A.G. Suits, *Science*. **274** (5292), 1508–1511 (1996). doi:10.1126/science.274.5292.1508
- [13] S. Datz, G. Sundström, C. Biedermann, L. Broström, H. Danared, S. Mannervik, J.R. Mowat and M. Larsson, *Phys. Rev. Lett.* **74** (6), 896 (1995). doi:10.1103/PhysRevLett.74.896
- [14] A.I. Florescu-Mitchell and J.B.A. Mitchell, *Phys. Rep.* **430** (5-6), 277–374 (2006). doi:10.1016/j.physrep.2006.04.002
- [15] S.E. Barlow, G.H. Dunn and M. Schauer, *Phys. Rev. Lett.* **52** (11), 902 (1984). doi:10.1103/PhysRevLett.52.902
- [16] D. Gerlich, *Physica Scripta*. **1995** (T59), 256 (1995). doi:10.1088/0031-8949/1995/T59/035
- [17] I.W. Smith, *Annu. Rev. Astron. Astrophys.* **49**, 29–66 (2011). doi:10.1146/annurev-astro-081710-102533
- [18] D. Field, N. Adams and D. Smith, *Mon. Not. R. Astron. Soc.* **192** (1), 1–10 (1980). doi:10.1093/mnras/192.1.1
- [19] R.A. Brownsword, I.R. Sims, I.W. Smith, D.W. Stewart, A. Canosa and B.R. Rowe, *Astrophys. J.* **485** (1), 195 (1997). doi:10.1086/3044402
- [20] J. Cernicharo, M. Agúndez, C. Cabezas, B. Tercero, N. Marcelino, J.R. Pardo and P. de Vicente, *Astron. Astrophys.* **649** (2021). doi:10.1051/0004-6361/202141156
- [21] I. Cherchneff, *Astron. Astrophys.* **545**, A12 (2012). doi:10.1051/0004-6361/201118542
- [22] J. Cernicharo, L. Waters, L. Decin, P. Encrenaz, A. Tielens, M. Agúndez, E. De Beck, H.S. Müller, J.R. Goicoechea and M.J. Barlow, *Astron. Astrophys.* **521**, L8 (2010). doi:10.1051/0004-6361/201015150
- [23] A.L. Mattioda, G.A. Cruz-Diaz, A. Ging, M. Barnhardt, C. Boersma, L.J. Allamandola, T. Schneider, J. Vaughn, B. Phillips and A. Ricca, *ACS Earth Space Chem.* **4** (12), 2227–2245 (2020). doi:10.1021/acsearthspacechem.0c00165
- [24] M. McCarthy, C. Gottlieb and P. Thaddeus, *Mol. Phys.* **101** (4-5), 697–704 (2003). doi:10.1080/0026897021000035197
- [25] Z. Yang, S. Doddipatla, R.I. Kaiser, A.A. Nikolayev, V.N. Azyazov and A.M. Mebel, *Astrophys. J. Lett.* **908** (2), L40 (2021). doi:10.3847/2041-8213/abde36
- [26] T. Yang, L. Bertels, B.B. Dangi, X. Li, M. Head-Gordon and R.I. Kaiser, *Proc. Natl. Acad. Sci. U.S.A.* **116** (29), 14471–14478 (2019). doi:10.1073/pnas.1810370116
- [27] R.I. Kaiser, *Chem. Rev.* **102** (5), 1309–1358 (2002). doi:10.1021/cr970004v
- [28] R.I. Kaiser, P. Maksyutenko, C. Ennis, F. Zhang, X. Gu, S.P. Krishtal, A.M. Mebel, O. Kostko and M. Ahmed, *Faraday Discuss.* **147**, 429–478 (2010). doi:10.1039/c003599h
- [29] T. Yang, B.B. Dangi, R.I. Kaiser, K.H. Chao, B.J. Sun, A.H.H. Chang, T.L. Nguyen and J.F. Stanton, *Angew. Chem. Int. Ed.* **56** (5), 1264–1268 (2017). doi:10.1002/anie.201611107
- [30] F. Zhang, S. Kim, R.I. Kaiser and A.M. Mebel, *J. Phys. Chem. A.* **113** (7), 1210–1217 (2009). doi:10.1021/jp807685v
- [31] Z. Yang, C. He, S. Goettl, R.I. Kaiser, V.N. Azyazov and A.M. Mebel, *J. Am. Chem. Soc.* **143** (35), 14227–14234 (2021). doi:10.1021/jacs.1c05510
- [32] M.W. Schmidt, K.K. Baldrige, J.A. Boatz, S.T. Elbert, M.S. Gordon, J.H. Jensen, S. Koseki, N. Matsunaga, K.A. Nguyen and S. Su, *J. Comput. Chem.* **14** (11), 1347–1363 (1993). doi:10.1002/jcc.540141112
- [33] H.J. Werner, P.J. Knowles, G. Knizia, F.R. Manby, M. Schütz, P. Celani, W. Gyröffy, D. Kats, T. Korona, and R. Lindh, *University of Cardiff Chemistry Consultants (UC3): Cardiff, Wales, UK* (2015).
- [34] J.-D. Chai and M. Head-Gordon, *Phys. Chem. Chem. Phys.* **10** (44), 6615–6620 (2008). doi:10.1039/b810189b
- [35] F. Jensen, *J. Chem. Theory Comput.* **10** (3), 1074–1085 (2014). doi:10.1021/ct401026a
- [36] N. Koga and K. Morokuma, *Chem. Phys. Lett.* **119** (5), 371–374 (1985). doi:10.1016/0009-2614(85)80436-X
- [37] J.N. Harvey and M. Aschi, *Phys. Chem. Chem. Phys.* **1** (24), 5555–5563 (1999). doi:10.1039/a907723e
- [38] C.M. Nunes, L.P. Viegas, S.A. Wood, J.P. Roque, R.J. McMahon and R. Fausto, *Angew. Chem. Int. Ed.* **59** (40), 17622–17627 (2020). doi:10.1002/anie.202006640
- [39] K.L. Gannon, M.A. Blitz, C.-H. Liang, M.J. Pilling, P.W. Seakins, D.R. Glowacki and J.N. Harvey, *Faraday Discuss.* **147**, 173–188 (2010). doi:10.1039/c004131a
- [40] T.B. Adler, G. Knizia and H.-J. Werner, *J. Chem. Phys.* **127** (22), 221106 (2007). doi:10.1063/1.2817618
- [41] G. Knizia, T.B. Adler and H.-J. Werner, *J. Chem. Phys.* **130** (5), 054104 (2009). doi:10.1063/1.3054300
- [42] K.A. Peterson, T.B. Adler and H.-J. Werner, *J. Chem. Phys.* **128** (8), 084102 (2008). doi:10.1063/1.2831537
- [43] J.B. Delos, *J. Chem. Phys.* **59** (5), 2365–2369 (1973). doi:10.1063/1.1680345
- [44] J.N. Harvey, *Phys. Chem. Chem. Phys.* **9** (3), 331–343 (2007). doi:10.1039/B614390C
- [45] A.W. Jasper, *J. Phys. Chem. A.* **119** (28), 7339–7351 (2015). doi:10.1021/jp512942w
- [46] S.J. Klippenstein, *J. Chem. Phys.* **96** (1), 367–371 (1992). doi:10.1063/1.462472
- [47] Z. Yang, C. He, S.J. Goettl, D. Paul, R.I. Kaiser, M.X. Silva and B.R. Galvão, *J. Am. Chem. Soc.* **144** (19), 8649–8657 (2022). doi:10.1021/jacs.2c01349
- [48] S.J. Sibener, R.J. Buss, P. Casavecchia, T. Hirooka and Y.T. Lee, *J. Chem. Phys.* **72** (8), 4341–4349 (1980). doi:10.1063/1.439714
- [49] H.F. Bettinger, P.v.R. Schleyer, H.F. Schaefer III, P.R. Schreiner, R.I. Kaiser and Y.T. Lee, *J. Chem. Phys.* **113** (10), 4250–4264 (2000). doi:10.1063/1.1286300
- [50] F. Zhang, Y. Guo, X. Gu and R.I. Kaiser, *Chem. Phys. Lett.* **440** (1-3), 56–63 (2007). doi:10.1016/j.cplett.2007.04.012
- [51] A. Berning, M. Schweizer, H.-J. Werner, P.J. Knowles and P. Palmieri, *Mol. Phys.* **98** (21), 1823–1833 (2000). doi:10.1080/00268970009483386
- [52] A.W. Jasper and J.A. Miller, *Combust. Flame.* **161** (1), 101–110 (2014). doi:10.1016/j.combustflame.2013.08.004
- [53] J. Troe, *Adv. Chem. Phys.* **101**, 817–852 (1997). doi:10.1021/jp962495d
- [54] Y. Georgievskii and S.J. Klippenstein, *J. Chem. Phys.* **122** (19), 194103 (2005). doi:10.1063/1.1899603

- [55] E. Herbst, *Chem. Soc. Rev.* **30** (3), 168–176 (2001). doi:10.1039/a909040a
- [56] E. Herbst, *Astrophys. J.* **252**, 810–813 (1982). doi:10.1086/159603
- [57] D. Smith, *Chem. Rev.* **92** (7), 1473–1485 (1992). doi:10.1021/cr00015a001
- [58] D. Gerlich and S. Horning, *Chem. Rev.* **92** (7), 1509–1539 (1992). doi:10.1021/cr00015a003
- [59] D. Gerlich and M. Smith, *Phys. Scr.* **73** (1), C25 (2005). doi:10.1088/0031-8949/73/1/N05
- [60] P. Armentrout and T. Baer, *J. Phys. Chem.* **100** (31), 12866–12877 (1996). doi:10.1021/jp953329t
- [61] M. Rodgers and P. Armentrout, *J. Am. Chem. Soc.* **122** (35), 8548–8558 (2000). doi:10.1021/ja001638d
- [62] H. Koizumi and P. Armentrout, *J. Chem. Phys.* **119** (24), 12819–12829 (2003). doi:10.1063/1.1627758
- [63] M. Kasha, *J. Chem. Phys.* **20** (1), 71–74 (1952). doi:10.1063/1.1700199
- [64] D.G. Fedorov, S. Koseki, M.W. Schmidt and M.S. Gordon, *Int. Rev. Phys. Chem.* **22** (3), 551–592 (2003). doi:10.1080/0144235032000101743
- [65] Z. Yang, C. He, S. Goettl and R.I. Kaiser, *J. Phys. Chem. A.* **125** (23), 5040–5047 (2021). doi:10.1021/acs.jpca.1c03023
- [66] A. Canosa, S. Le Picard, S. Gougeon, C. Rebrion-Rowe, D. Travers and B. Rowe, *J. Chem. Phys.* **115** (14), 6495–6503 (2001). doi:10.1063/1.1396855
- [67] S.C. Basu and D. Husain, *J. Photochem. Photobiol., A.* **42** (1), 1–12 (1988). doi:10.1016/1010-6030(88)80044-3
- [68] G. Vanuzzo, N. Balucani, F. Leonori, D. Stranges, S. Falcinelli, A. Bergeat, P. Casavecchia, I. Gimondi and C. Cavallotti, *J. Phys. Chem. Lett.* **7** (6), 1010–1015 (2016). doi:10.1021/acs.jpcllett.6b00262
- [69] G. Vanuzzo, A. Caracciolo, T.K. Minton, N. Balucani, P. Casavecchia, C. de Falco, A. Baggioli and C. Cavallotti, *J. Phys. Chem. A.* **125** (38), 8434–8453 (2021). doi:10.1021/acs.jpca.1c06913
- [70] A.M. Schmoltner, S.Y. Huang, R.J. Brudzynski, P.M. Chu and Y.T. Lee, *J. Chem. Phys.* **99** (3), 1644–1653 (1993). doi:10.1063/1.465334
- [71] F. Salama, E. Bakes, L. Allamandola and A. Tielens, *Astrophys. J.* **458**, 621 (1996). doi:10.1086/176844
- [72] A.G.G.M. Tielens, *Annu. Rev. Astron. Astrophys.* **46**, 289–337 (2008). doi:10.1146/annurev.astro.46.060407.145211
- [73] L.J. Allamandola, A.G.G.M. Tielens and J.R. Barker, *Astrophys. J. Suppl.* **71**, 733–775 (1989). doi:10.1086/191396